THE ASTROPHYSICAL JOURNAL, 459:L91–L94, 1996 March 10

MASS-LUMINOSITY RELATIONSHIP AND LITHIUM DEPLETION FOR VERY LOW MASS STARS

GILLES CHABRIER AND ISABELLE BARAFFE
Centre de Recherche Astrophysique de Lyon (UMR 147 CNRS), Ecole Normale Supérieure, 69364 Lyon Cedex 07, France;
chabrier@cral.ens-lyon.fr, baraffe@cral.ens-lyon.fr

AND

BERTRAND PLEZ
Niels Bohr Institute, Blegdamsvej 17, DK 2100 Copenhagen, Denmark; plez@nbi.dk
Received 1995 November 1; accepted 1996 January 2

ABSTRACT

We derive mass-luminosity relationships for very low mass stars ($0.06 < m/M_{\odot} < 0.6$) for different metallicities. Calculations are conducted with the different nongray atmosphere models presently available to illustrate the uncertainties in the stellar models. The theoretical mass-magnitude relation reproduces accurately the *observed* relationship in the V band (Henry & McCarthy) but still underestimates the flux in the K band by $\sim$0.5 mag, a consequence of the still inaccurate water opacities. Calculations based on the gray approximation are shown to yield incorrect results over the entire mass range of interest. We also show that the fate of objects near the hydrogen-burning limit depends significantly on the treatment of the atmosphere. Nongray effects yield cooler and less luminous objects for a given mass near the stellar/substellar transition, and thus a *lower* hydrogen-burning minimum mass, $m \approx 0.07\ M_{\odot}$, for solar metallicity.

The depletion of lithium along evolution is considered in detail, and we give age versus lithium-abundance relations that provide useful guides to determine the mass and the age of spectroscopically observed low-mass objects.

Subject headings: stars: evolution — stars: low-mass, brown dwarfs — stars: luminosity function, mass function

1. INTRODUCTION

The derivation of reliable very low mass star (VLMS) models is essential to accurately characterize the *mass* of these objects and to identify genuine brown dwarfs. For this reason, one of the ultimate goals of VLMS theory is the derivation of an accurate *mass-luminosity* relationship, the cornerstone for deriving reliable mass functions from the observed luminosity functions and to identify the nature of dark matter in the disks and halos of spiral galaxies.

Recently, Baraffe et al. (1995) derived new evolutionary models for low-mass stars, including the best input physics presently available. These models reproduce the *observations* of Population I and II VLMSs in color-magnitude diagrams (Monet et al. 1992), and all the observed parameters of the two eclipsing binary systems CM Draconis and YY Geminorum (Chabrier & Baraffe 1995a, b). Such comparisons with observations reinforce the validity of these models to describe the structural and thermal properties of VLMSs with reasonable accuracy.

The aim of the present Letter is to derive mass-luminosity (m-L) relationships for VLMSs and to examine the uncertainties in the present models. We also examine the effect of lithium depletion along evolution because the presence of this element is a key diagnostic for identifying substellar objects.

2. INPUT PHYSICS

The inputs for the model of the structure and the evolution of VLMSs include the equation of state (EOS), the screening corrections to the thermonuclear reaction rates, and nongray model atmospheres. We use the Saumon-Chabrier EOS (Saumon & Chabrier 1991, 1992; Saumon, Chabrier, & Van Horn 1995) especially devoted to the description of dense stellar interiors, i.e., $m \lesssim 0.6\ M_{\odot}$. The screening corrections to thermonuclear reaction rates include the ion screening *and* the effect of electron polarization (Chabrier 1995).

Tremendous progress has been made recently in model atmosphere and synthetic spectra calculations for cool M dwarfs at zero (Saumon et al. 1994) and finite metallicity (Allard & Hauschildt 1995, hereafter AH95; Brett 1995a, hereafter B95; Brett 1995b). Some differences still persist between these models (see, e.g., Bessell 1995), and we conducted evolutionary calculations with both AH95 (the so-called *Base* models) and B95[1] model atmospheres, and also with the next generation of the Allard & Hauschildt models (Allard et al. 1996), labeled NG2. The B95 and NG2 models are presently available for solar abundances only, restricting the domain of comparison to this particular, but most important, metallicity. Calculations for metal-depleted abundances rely on the AH95 models. The main differences between these different sets of models stem essentially from (see the mentioned publications for further details) (1) different techniques in the opacity calculations: the AH95 ($\equiv$ *Base*) models are based on the straight-mean (SM) approximation, whereas B95 and NG2 use the more accurate opacity-sampling (OS) technique; (2) different line lists, especially for TiO, the main source of absorption below $T_{\rm eff} \sim 3500$ K in the optical: the line list computed by Plez, Brett, & Nordlund (1992) for B95 and the one from Jørgensen (1994) in NG2; and (3) the use in B95 of a pseudo–line list for H_2O based on old SM data (cf. Plez et al. 1992), while AH95 use the original SM tables (see

[1] Models of B95 were available only for $T_{\rm eff} \geq 3000$ K and [M/H] = 0, but J. Brett kindly provided us with opacity updates (especially CaH) that allowed us to compute a few models at $T_{\rm eff}$ down to 2200 K.

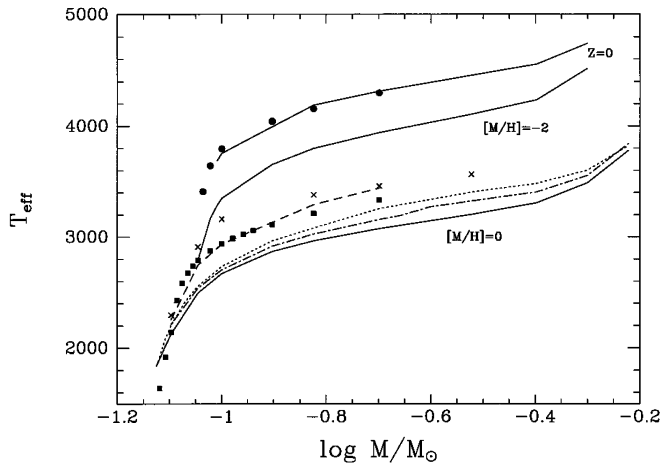

FIG. 1.—Mass–effective temperature diagram at $t = 5$ Gyr. *Solid lines*: models based on Saumon et al. (1994) atmosphere models for $Z = 0$ and on AH95 (*Base*) atmosphere models for [M/H] = −2 and 0, from top to bottom. *Dashed lines*: models based on gray approximation (with the Alexander & Fergusson (1994) Rosseland opacities), as in previous studies, for [M/H] = 0. *Dash-dotted line*: models based on B95. *Dotted line*: models based on NG2 for [M/H] = 0. Comparisons are made with the most recent VLMS models. *Full squares*: BHSL93. *Crosses*: D'Antona & Mazzitelli (1994), both based on a gray approximation at [M/H] = 0. *Solid circles*: Saumon et al. (1994) nongray models at $Z = 0$. The initial helium abundance is $Y = 0.275$ for solar metallicity, $Y = 0.23$ for [M/H] = −2, and $Y = 0.25$ for $Z = 0$ (to compare with Saumon et al. 1994).

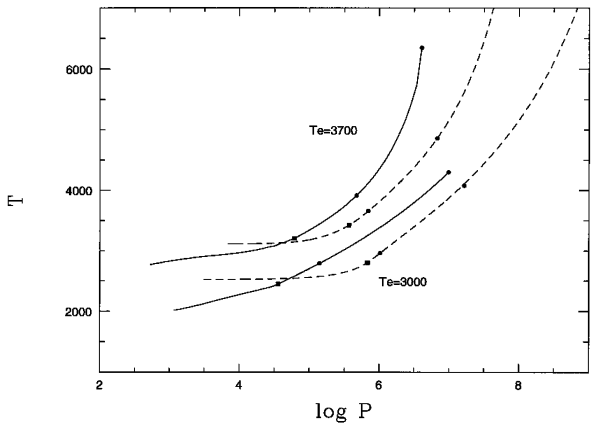

FIG. 2.—$T(P)$ atmosphere profiles at $T_{eff} = 3000$ and 3700 K, log $g = 5$, [M/H] = 0. *Solid lines*: B95 nongray models. *Dotted line*: Eddington approximation [$q(\tau) = 2/3$]. *Solid circles*: $\tau = \frac{2}{3}$ and $\tau = 100$. *Solid squares*: location of the onset of convection in the atmosphere.

AH95) and NG2 use the more recent OS tables from Jørgensen (1994).

Since the two sets of models (Allard and collaborators vs. Brett and Plez) derive from two *independent sources*, including the model atmosphere code itself, the present comparisons provide the best estimate of present uncertainties in VLMS stellar models.

In a previous Letter (Baraffe et al. 1995), we showed the necessity of using *synthetic spectra* for reliable comparison with observed *colors* and *magnitudes* of M dwarfs. In the present Letter, we emphasize the need to use accurate *boundary conditions* (gray vs. nongray) between the atmosphere and the interior structure along evolution. A complete description of the calculations will be presented elsewhere (Chabrier & Baraffe 1995a).

3. RESULTS

Calculations have been performed over the mass range $0.06 \leq m/M_\odot \leq 0.6$ for different metallicities. Convection is described according to the mixing-length theory with a mixing-length parameter $l_{mix}/H_P = 1$ in the stellar interior. Within the aforementioned mass range, variations of this parameter around this value do not affect the results significantly. All models were evolved from the initial deuterium-burning phase to an age of 5 Gyr. The age of the zero-age main sequence, defined as the stage where the star achieves thermal equilibrium ($dL/dm \approx \varepsilon_{nuc}$), varies from $\sim 10^8$ yr for a 0.6 $M_\odot$ to $\sim 5 \times 10^9$ yr for $m > 0.07$ $M_\odot$, for any metallicity, so that all the objects presented in these calculations lie on the MS.

m-L and m-T_{eff} relations.—The *m*-T_{eff} relations for different metallicities are displayed in Figure 1. An interesting analysis arises from the comparison with the most recent models of Burrows et al. (1993, hereafter BHSL93), who solved explicitly the radiative transfer equations (no diffusion approximation) but used *gray* atmosphere models. As shown by Allard (1990) and Saumon et al. (1994), deep inside the atmosphere (optical depth $\tau \gg 1$), nongray models are systematically hotter than the gray ones, *for a given effective temperature and surface gravity*. This is illustrated in Figure 2, which displays atmosphere profiles in *T-P* for gray models [within the Eddington approximation $q(\tau) = \frac{2}{3}$] and nongray models. In the outermost layers of the atmosphere, the nongray models are *cooler* than the gray ones, as a result of molecular blanketing (surface cooling). The situation gradually reverses in the deeper layers because of the back-warming. Also shown in Figure 2 are the locations of different optical depths that correspond to different boundary layers between the interior and atmosphere profiles (*solid circles*) and the location of the onset of convection in the atmosphere (*solid squares*). The value $\tau = \frac{2}{3}$ corresponds to the standard boundary condition, whereas $\tau = 100$ is the value used in the present calculations (this corresponds to ~99% of the stellar radius, so that $L = 4\pi R^2 \sigma T_{eff}^4$ is well verified). As clearly shown in Figure 1, using a gray approximation requires a *larger* T_{eff} for the same (τ, log g). The gray approximation as a boundary condition fails below $T_{eff} \sim 4000$ K, i.e., over the *entire* M-dwarf characteristic mass range, a direct consequence of the ongoing H_2 molecular dissociation and the resulting penetration of convection in the outer part of the atmosphere (see, e.g., Dorman, Nelson, & Chau 1989; Saumon et al. 1994; Baraffe et al. 1995). Stellar models based on this approximation severely *overestimate* the luminosity and the effective temperature for a given mass, or conversely yield *smaller masses* for a given luminosity and/or temperature, in the stellar domain.

As also shown in Figure 1, the gray approximation predicts too steep a slope in the *m-L* relation near the *bottom* of the stellar mass distribution, which yields too large a hydrogen-burning minimum mass (HBMM) (for $Z = Z_\odot$). This is illustrated in Figure 3, which displays the evolution of a 0.075 $M_\odot$ star with solar metallicity. Within the Eddington approximation, the more luminous object cannot reach thermal equilibrium for this mass ($L_{nuc}/L < 1$), whereas it does with a (less luminous) nongray atmosphere. To make sure such a difference does not stem from the onset of grain formation (not included in present nongray atmosphere models), we have computed evolutionary calculations with *grainless* Rosseland opacities, kindly provided by D. Alexander. Although some differences appear below $T_{eff} \approx 1800$ K, as expected, the brown

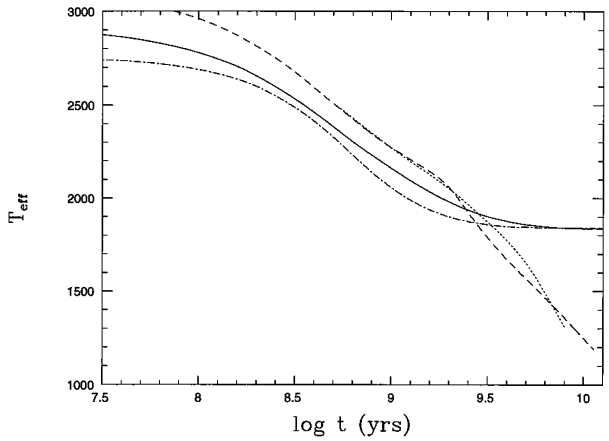

FIG. 3.—Evolution of $T_{\rm eff}$ as a function of time for a 0.075 $M_\odot$ with $Z = Z_\odot$. *Solid line*: results based on NG2 nongray atmosphere models. *Dot-dashed line*: results based on AH95 (*Base*) nongray atmosphere models. *Dashed line*: Eddington approximation with the Alexander & Fergusson (1994) Rosseland opacities. *Dotted line*: same as dashed line with *grainless* opacities.

dwarf limit still occurs for the same conditions. In fact, the fate of the star is determined long before this limit, namely, near $T_{\rm eff} \sim 2500$ K. These detailed comparisons demonstrate convincingly that calculations based on boundary conditions derived from a gray approximation yield erroneous evolutionary models for VLMS, down to the hydrogen-burning limit. This stresses the importance of using accurate nongray models *and* boundary conditions to derive reliable models. The HBMM obtained with the present models (with any nongray atmosphere model; cf. Fig. 3) is $m \approx 0.07$ $M_\odot$ (respectively, $m \approx 0.088$ $M_\odot$) for [M/H] = 0 (respectively, [M/H] = −2), which corresponds to $M_V = 21.5$ (respectively, $M_V = 14.7$) for $t = 1$ Gyr (about 3 more dex for $t = 5$ Gyr). More precise determinations require nongray atmosphere models with grain formation.

Comparison between different nongray atmosphere models.—In Figure 4 we compare the theoretical m-M_V relationships obtained with the atmosphere models of AH95, NG2, and B95 (for solar metallicity) with the observational fit derived by Henry & McCarthy (1993, hereafter HMC93). We note the excellent agreement between the observation and the stellar models based on B95 and NG2, while models based on AH95 clearly underestimate the flux at this wavelength. This illustrates the improvement in the treatment of TiO and H_2O opacities. Such accuracy between theory and observation is not reached in the K band, as confirmed by Tinney et al. (1995). While the general trend, i.e., the slope of the m-L relation, is reasonably well reproduced by the theory, the magnitudes M_K of the *three different types of stellar models* are almost indistinguishable and lie ∼0.5 mag fainter than the empirical fit for $m \lesssim 0.5$ $M_\odot$ ($T_{\rm eff} \lesssim 3500$ K). This very likely arises from the still inaccurate H_2O opacities presently used in all atmosphere models (see, e.g., AH95 and B95). These comparisons illustrate the significant improvement in the modeling of low-mass stars accomplished recently by the inclusion of improved EOS and atmosphere models.

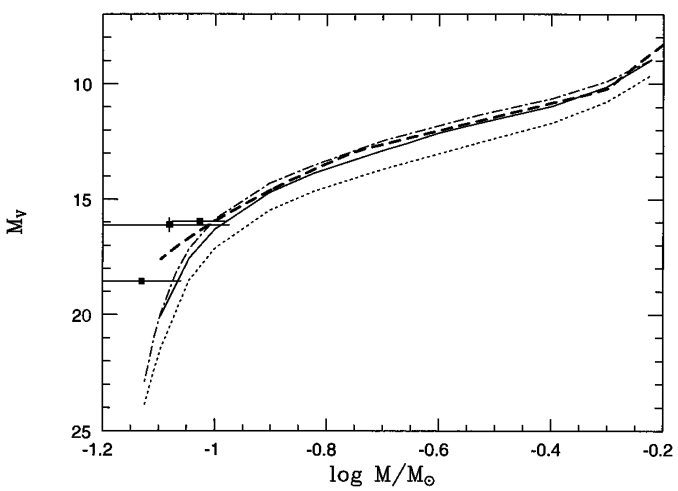

FIG. 4.—Mass-M_V relation. The thick dashed line is the fitted relation of HMC93. *Solid line*: results based on the B95 model atmospheres. *Dot-dashed line*: results based on the NG2 model atmospheres. *Dotted line*: results based on the AH95 model atmospheres. All for [M/H] = 0. *Squares*: the three least massive objects from HMC93.

We recall that the HMC93 fits, as acknowledged by the authors themselves, rely on intermediate disk objects, without consideration of age or metallicity dispersion. The present comparison with the observations of HMC93 has been done for solar metallicity and an age $t = 5$ Gyr, so that *all* H-burning objects ($m > 0.07$ $M_\odot$) lie on the MS. A detailed study of metallicity effects around the aforementioned solar value would not be meaningful for two reasons: (1) a Δ[M/H] = 0.5 in the model translates to a $\Delta M \approx 0.5$ mag in absolute magnitude for all passbands, which is of the order of the observational dispersion around each metal class (Legget 1992), and (2) the limited sample of small-mass stars does not permit a detailed analysis (HMC93).

The age effect deserves more investigation because it modifies the faint (low-mass) end of the m-L relation. Calculations at $t = 1$ Gyr affect only objects below $m = 0.08$ $M_\odot$, which at this age are still on the pre-MS contraction phase. Therefore, for masses $m \gtrsim 0.08$ $M_\odot$ ($M_V \lesssim 20$), the m-L relationship remains unaffected after $t = 1$ Gyr. The three least massive objects observed by HMC93 deserve peculiar attention. *All* of these three objects show chromospheric *and* coronal activity that strongly suggest a young age (Flemings, Schmitt, & Giampapa 1995). They could then be more luminous than the model predictions at 1 Gyr. Indeed, a m-L relation derived from models at $t = 0.5$ Gyr lies right in the middle of the error bars.

The theoretical mass-M_V relation, based on B95 and NG2 atmosphere models for *solar metallicity*, is well fitted, within the 0.075–0.6 $M_\odot$ mass range, by the simple polynomial expression $\log (m/M_\odot) \approx aM_V^3 + bM_V^2 + cM_V + d$.[2]

The difference, for $Z = Z_\odot$, between the AH95 models and the NG2 or B95 models is ∼6% in $T_{\rm eff}$ and ∼20% in $L/L_\odot$, i.e., ∼0.5 mag in M_V. Assuming the differences are similar for subsolar metallicities (probably smaller, given the decreasing abundance of "metallic" molecules), this states the present uncertainty in VLMS stellar models, for subsolar metallicities.

Lithium depletion.—Detailed results concerning the depletion and the minimum-burning masses of the light elements Li, Be, and B will be presented in a forthcoming paper (Chabrier & Baraffe 1995). In this Letter, we focus on the depletion of Li along evolution because the presence of Li in a faint object is a key diagnostic for identifying its *substellar* nature (Rebolo, Martín, & Magazzù 1992; Martín, Rebolo, & Magazzù 1994; Basri, Marcy, & Graham 1995).

[2] $a = -6.8796 \times 10^{-4}$, $b = 4.1979 \times 10^{-2}$, $c = -0.86207$, $d = 4.8580$ for $22.7 < M_V < 11.3$ ($0.075 \leq m/M_\odot \leq 0.3$) and $a = -8.3150 \times 10^{-4}$, $b = -4.1465 \times 10^{-3}$, $c = 0.21495$, and $d = -1.2135$ for $11.3 < M_V < 9$ ($0.3 < m/M_\odot \leq 0.6$).

TABLE 1

CHARACTERISTICS OF THE MODELS[a]

$M/M_\odot$	t (10^8 yr)	$T_{\rm eff}$	$L/L_\odot$	M_V	M_I	M_K
0.060.....	2.554	2347	−3.41	18.36	14.28	10.17
	9.994	1732	−4.15	23.58	17.36	12.10
0.070.....	1.271	2694	−2.97	15.52	12.35	9.21
	2.233	2562	−3.19	16.68	13.19	9.71
0.075.....	1.057	2771	−2.85	14.93	11.92	8.95
	1.746	2686	−3.03	15.72	12.52	9.36
0.080.....	0.911	2829	−2.75	14.50	11.58	8.73
	1.445	2769	−2.91	15.10	12.07	9.10
0.090.....	0.696	2915	−2.59	13.84	11.06	8.37
	1.078	2877	−2.73	14.31	11.45	8.70
0.100.....	0.580	2994	−2.45	13.30	10.63	8.06
	0.877	2957	−2.58	13.74	11.01	8.39
0.200.....	0.265	3250	−1.75	11.08	8.72	6.40
	0.375	3259	−1.86	11.31	8.96	6.67
0.300.....	0.184	3324	−1.41	10.14	7.83	5.53
	0.261	3357	−1.50	10.28	8.02	5.78
0.400.....	0.137	3395	−1.15	9.43	7.17	4.89
	0.197	3411	−1.25	9.63	7.40	5.16
0.500.....	0.108	3499	−0.93	8.79	6.61	4.34
	0.161	3501	−1.05	9.04	6.88	4.66
0.600.....	0.091	3585	−0.76	8.29	6.17	3.93
	0.162	3595	−0.93	8.63	6.54	4.38

[a] The initial Li abundance ($[{\rm Li}]_0 = 10^{-9}$) has been depleted by a factor 2 (*upper row*) and 100 (*lower row*) for [M/H] = 0.

Li burning requires central temperatures ~2–3 × 10^6 K, i.e., $t \lesssim 10^8$ yr for $m \gtrsim 0.06\ M_\odot$. Table 1 displays the age for which the initial Li abundance has been decreased by a factor 2 and 100 in the mass range 0.06–0.6 $M_\odot$. Stars older than the age corresponding to a factor 100 in depletion are unlikely to exhibit Li features in their spectra. Recall, however, that the predicted magnitudes (especially I and K) have to be taken with some (~0.5 mag) uncertainty. Uncertainties in these ages related to the different, most recent atmosphere models (NG2 vs. B95) are less than 5%. We recall that those ages are not affected by the treatment of the convection in the stellar interior and the variation of the mixing-length parameter, at least for masses $m < 0.4\ M_\odot$, for which the star is entirely convective. Note that the age in Table 1 decreases with metallicity: lower metallicities yield larger luminosities and temperatures for a given mass, and then shorter times to reach the Li-burning temperature.

4. CONCLUSION

In this Letter, we have derived m-L relationships for VLMSs for various metallicities. The present study stresses the importance of using nongray atmospheres *and* accurate boundary conditions to derive reliable m-L relationships for VLMSs, and to determine accurately the limit between the stellar and substellar domains. Stellar models based on nongray atmospheres are shown to evolve at lower $T_{\rm eff}$ and lower luminosity than gray models, for solar metallicity, yielding a lower hydrogen-burning minimum mass. Because of the effect of dust absorption below ~1800 K (see Fig. 3), and the lack of nongray atmosphere models with grains, the new HBMM cannot be derived accurately yet but is presently found to be ~0.07 $M_\odot$ for solar metallicity and ~0.088 $M_\odot$ for [M/H] = −2.

The stellar models based on B95 and NG2 are shown to reproduce accurately, for the first time, the observational mass-magnitude relation in the V band. This stems undoubtedly from the more accurate treatment of TiO absorption with the OS technique. The models accurately reproduce, in particular, the observed rapid drop in luminosity near the bottom of the stellar mass distribution. This assesses the validity of these models, which include the most updated physics presently available, to derive reliable mass functions from observed luminosity functions in the V band (Méra, Chabrier, & Baraffe 1996). All models fail to reproduce the observed magnitudes for a given mass in the K band by ~0.5 mag, below ~0.5 $M_\odot$, i.e., $T_{\rm eff} \approx 3500$ K, most certainly a consequence of the inaccurate water opacities. They do, however, reproduce accurately the general trend, i.e., the *slope* of the m-M_K relation. These results clearly illustrate the uncertainty in the present stellar models for VLMSs. Agreement between theory and observation is now reaching *quantitative* levels and provides a reliable mass determination in the V band, whereas further improvement is still needed in infrared bandpasses.

Finally, we analyze the lithium depletion along evolution and give various [Li]-age relations for the mass range of interest. These relations provide useful guides to determine the mass of the faintest objects observed presently and, in particular, to identify genuine brown dwarfs.

The authors gratefully acknowledge France Allard, Peter Hauschildt, and John M. Brett for providing atmosphere models and spectra prior to publication, and the latter for also kindly updating our opacities and MARCS code. We are also thankful to Dave Alexander, for computing grainless opacities upon request, and Didier Saumon, for allowing us to generate calculations with his atmosphere models. B. P. is supported by a HCM grant from the Commission of the European Communities.

REFERENCES

Allard, F. 1990, Ph.D. thesis, Univ. Heidelberg
Allard, F., Alexander, D. R., Hauschildt, P. H., & Schweitzer, A. 1996, ApJ, submitted
Allard, F., & Hauschildt, P. H. 1995, ApJ, 445, 433 (AH95)
Alexander, D. R., & Fergusson, J. W. 1994, ApJ, 437, 879
Baraffe, I., Chabrier, G., Allard, F., & Hauschildt, P. 1995, ApJ, 446, L35
Basri, G., Marcy, G. W. M., & Graham, J. R., 1995, ApJ, submitted
Bessell, M. S. 1995, in The Bottom of the Main Sequence and Beyond, ed. C. G. Tinney (Berlin: Springer), 123
Brett, J. M. 1995a, A&A, 295, 736 (B95)
———. 1995b, A&AS, 109, 263
Burrows A., Hubbard, W. B., Saumon, D., & Lunine, J. I. 1993, ApJ, 406, 158 (BHSL93)
Chabrier, G. 1995, in preparation
Chabrier, G., & Baraffe, I. 1995a, in preparation
———. 1995b, ApJ, 451, L29
D'Antona, F., & Mazzitelli, I. 1994, ApJS, 90, 467
Dorman, B., Nelson, L. A., & Chau, W. Y. 1989, ApJ, 342, 1003
Flemings, T. A., Schmitt, J. H. M. M., & Giampapa, M. S. 1995, ApJ, 450, 401
Henry, T. D., & McCarthy, D. W., Jr. 1993, AJ, 106, 773 (HMC93)
Jørgensen, U. G. 1994, ApJ, 284, 179
Kroupa, P., Tout, C. A., & Gilmore, G. 1990, MNRAS, 244, 76
Leggett, S. K. 1992, ApJS, 82, 351
Martín, E. L., Rebolo, R., & Magazzù, A. 1994, ApJ, 436, 262
Méra, D., Chabrier, G., & Baraffe, I., 1996, ApJ, in press
Monet, D. G., Dahn, C. C., Vrba, F. J., Harris, H. C., Pier, J. R., Luginbuhl, C. B., & Ables, H. D. 1992, AJ, 103, 638
Plez, B., Brett, J. M., & Nordlund, A. 1992, A&A, 256, 551
Rebolo, R., Martín, E. L., & Magazzù, A. 1992, ApJ, 389, 83
Saumon, D., Bergeron, P., Lunine, L. I., Hubbard, W. B., & Burrows, A. 1994, ApJ, 424, 333
Saumon, D., & Chabrier, G. 1991, Phys. Rev. A, 44, 5122
———. 1992, Phys. Rev. A, 46, 2084
Saumon, D., Chabrier, G., & Van Horn, H. M. 1995, ApJS, 99, 713
Tinney, C. C., et al. 1995, preprint